Fig. 1. Examples of curved wires (a) helix (b) wire loop (c) meander line.
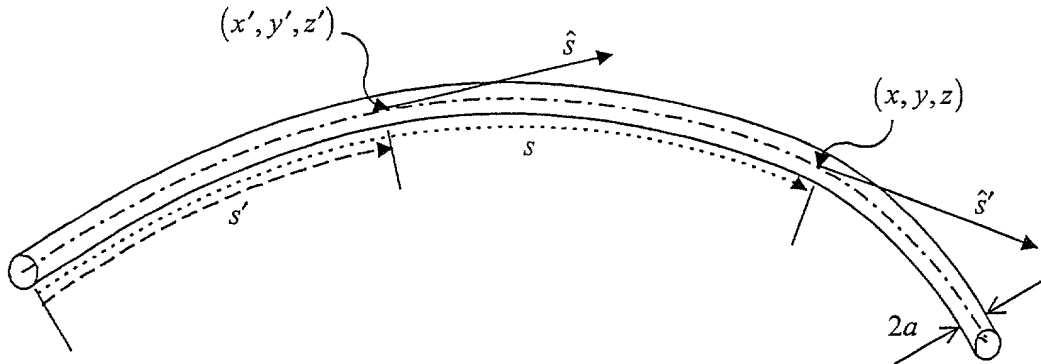

Fig. 2. Arbitrary curved wire of radius a with source point, observation point, and unit vectors.
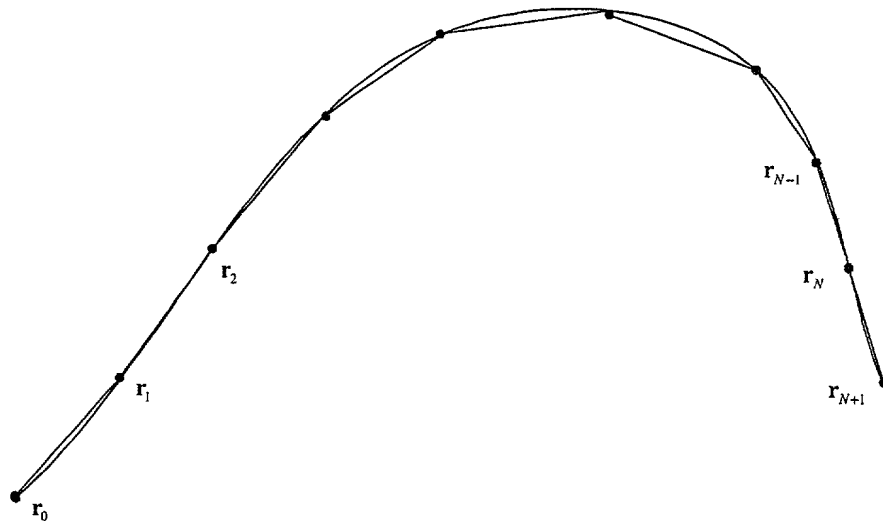

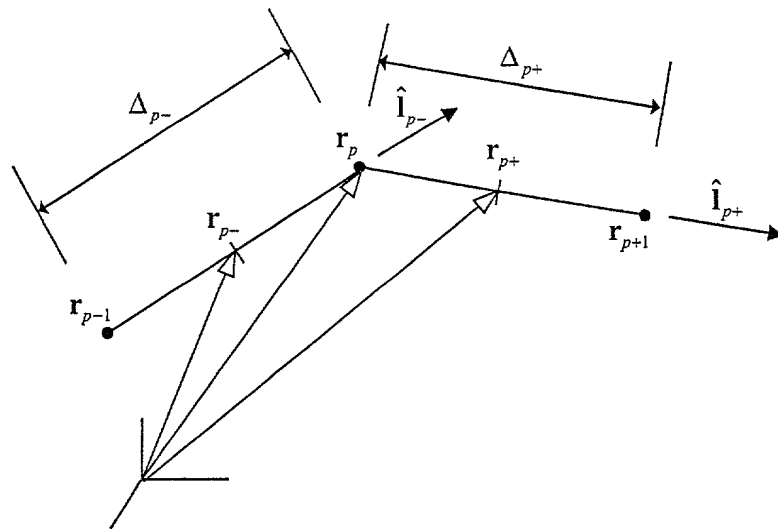Fig. 3. Straight line segment approximation of curved-wire axis.

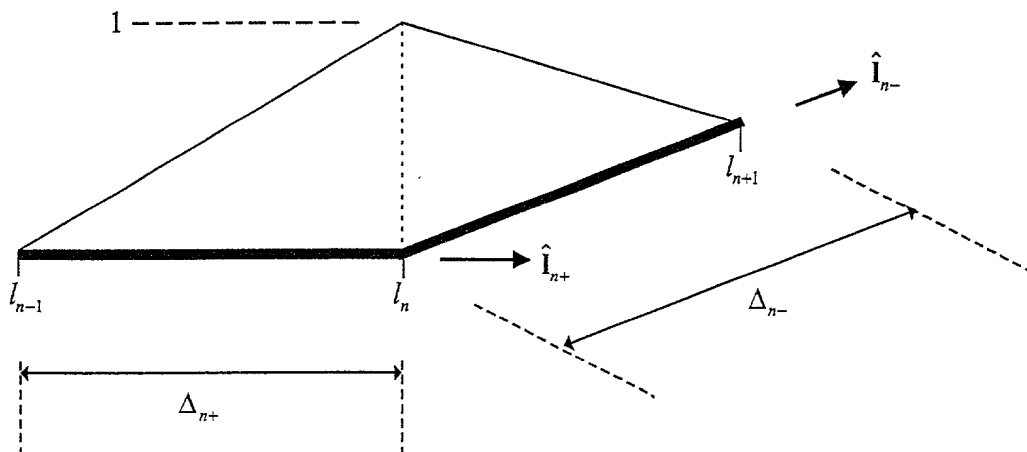Fig. 4. Geometrical parameters for adjacent straight line segments.
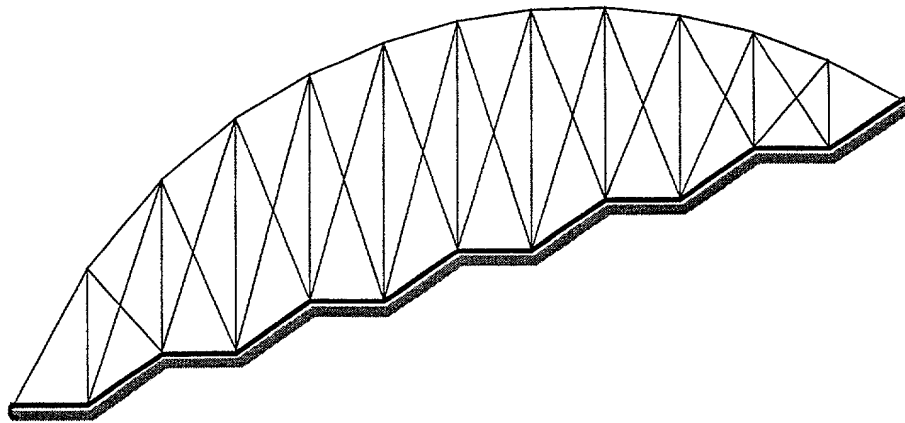

Fig. 5. Triangular basis function Λ_n.

Fig. 6. Piecewise linear expansion of the current along a meander line.
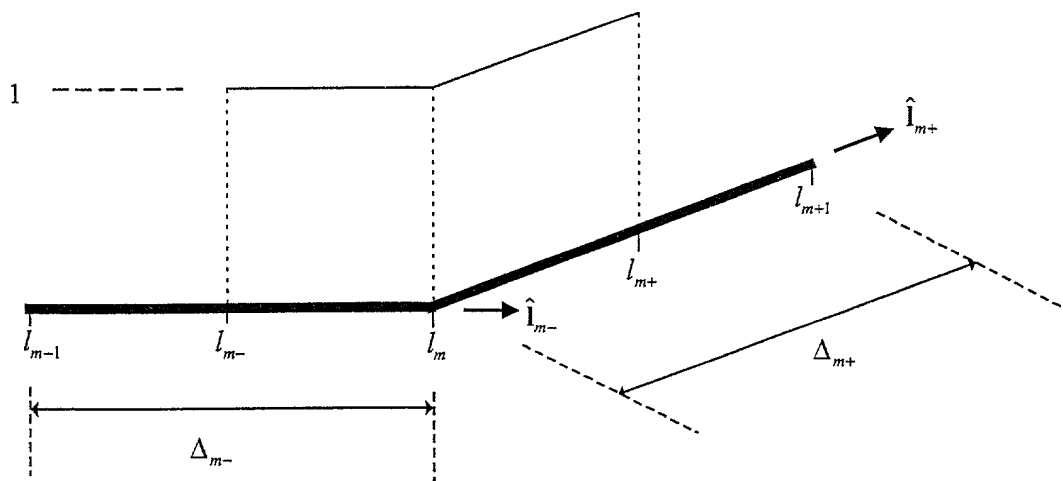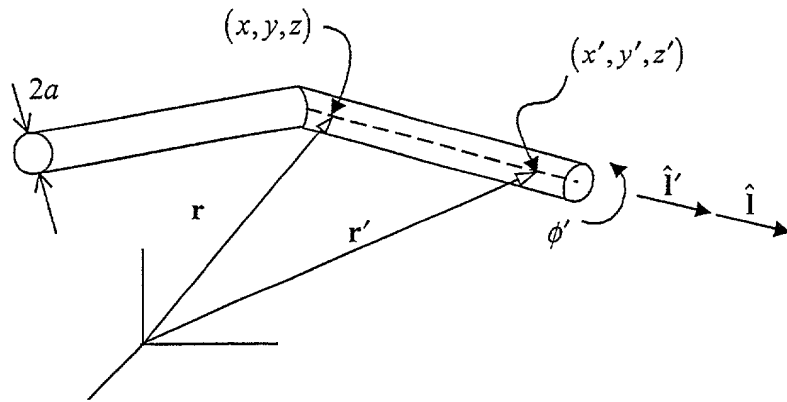

Fig. 7. Testing pulse Π_m.

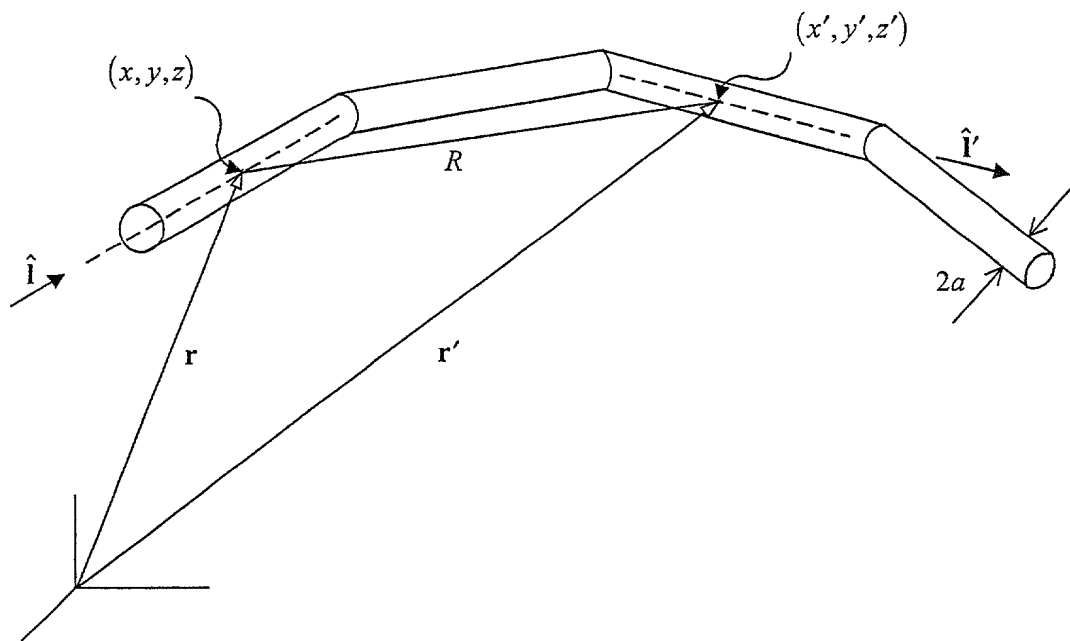Fig. 8. Source and observation points on adjacent straight-wire segments.

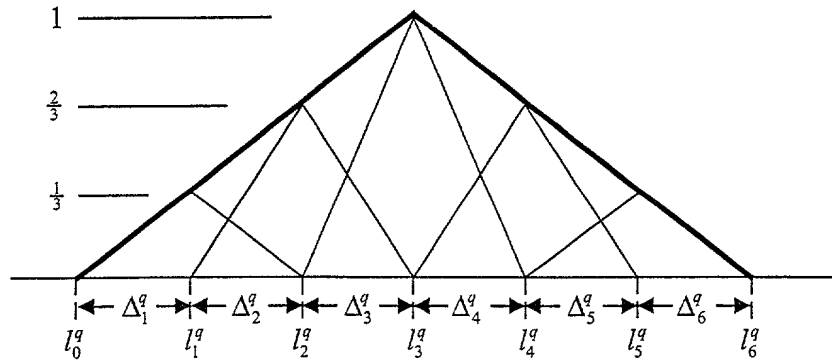Fig. 9. Source and observation points on different linear wire segments.

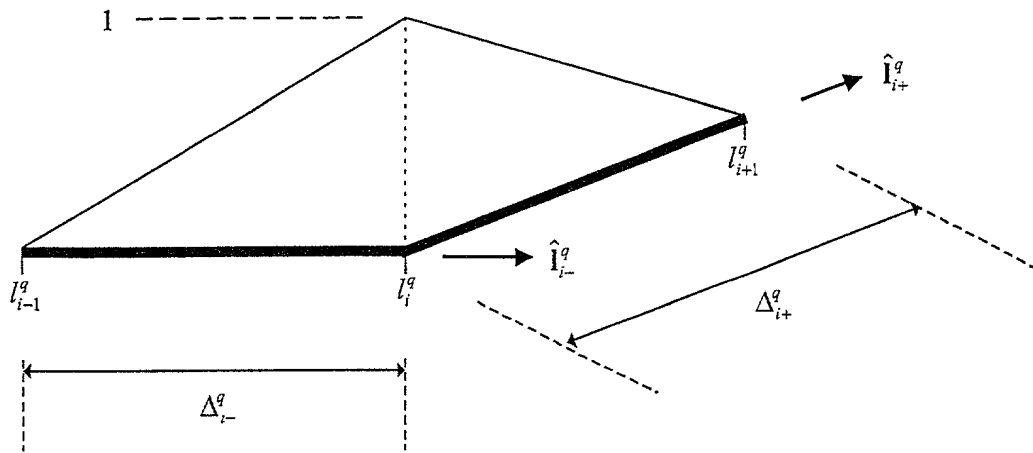Fig. 10. Composite triangle basis function $\widetilde{\Lambda}_q$ with five constituent triangles.
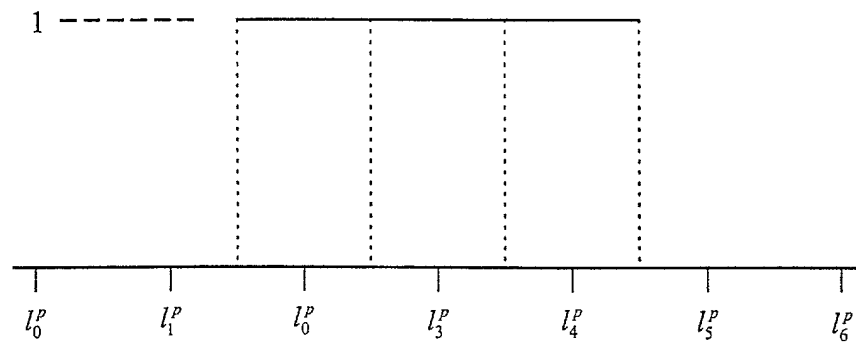

Fig. 11. Constituent triangle Λ_i^q.

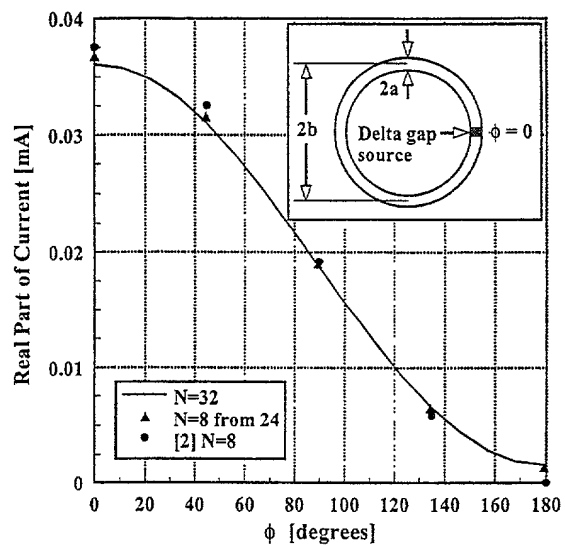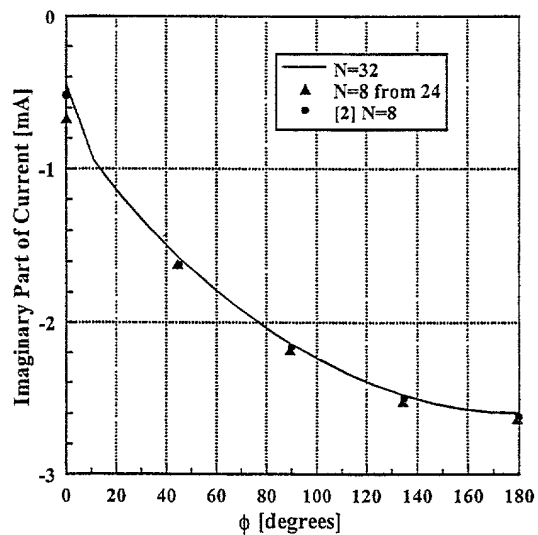
Fig. 12. Composite testing pulse $\widetilde{\Pi}_p$.

Fig. 13. Constituent testing pulse Π_k^p.

Fig. 14. Current expansion with composite basis functions.

(a)

(b)

Fig. 15.(a) Real part of current on wire loop antenna; (b) Imaginary part of current ($a = 0.0027\lambda$, $b = 0.0637\lambda$).
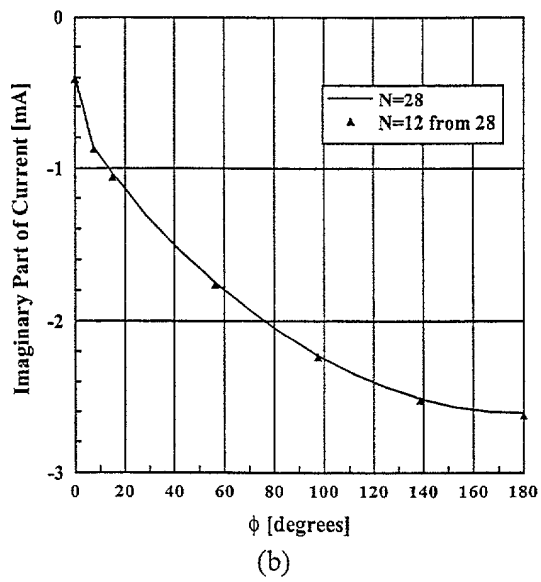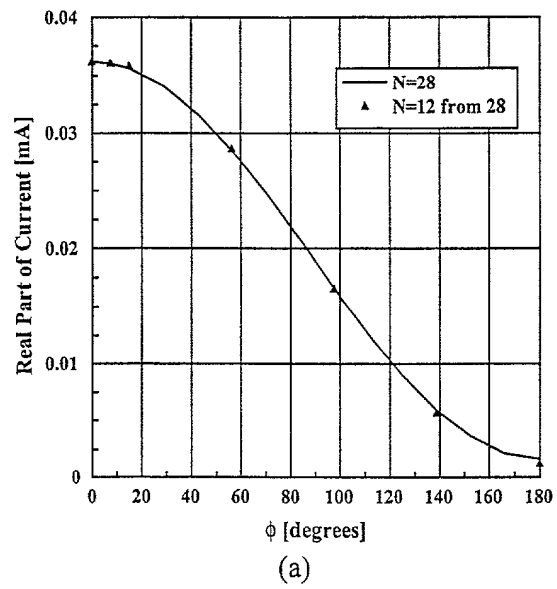
Fig. 16. (a) Real part of current on wire loop antenna of Fig. 15 without composite basis function at source; (b) Imaginary part of current.
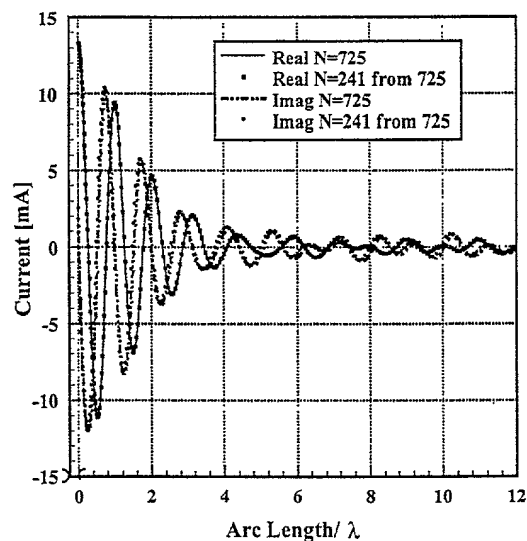
Fig. 17. Mode 2 current on one arm of four arm Archimedian spiral antenna (spiral constant 0.02λ, arm length 12λ, wire radius 0.006λ).
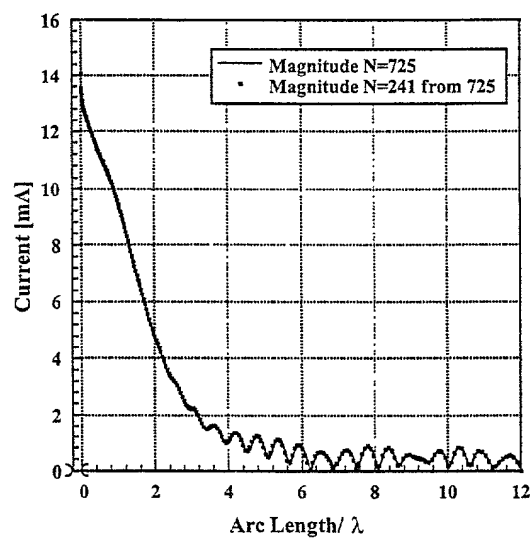

Fig. 18. Magnitude of mode 2 current on one arm of four arm Archimedian spiral antenna (spiral constant 0.02λ, arm length 12λ, wire radius 0.006λ).
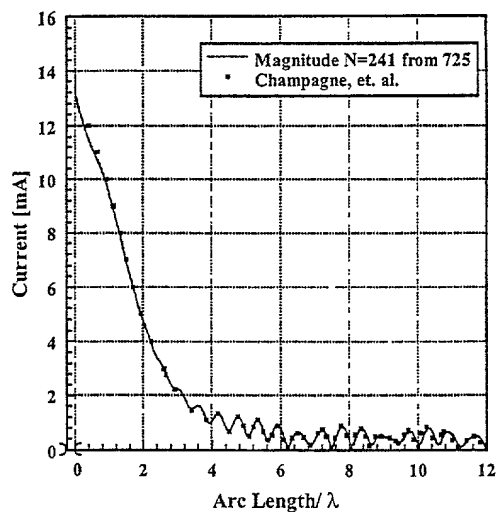
Fig. 19. Magnitude of mode 2 current on one arm of four arm Archimedian spiral antenna with data of [2] for comparison (spiral constant 0.02λ, arm length 12λ, wire radius 0.006λ).
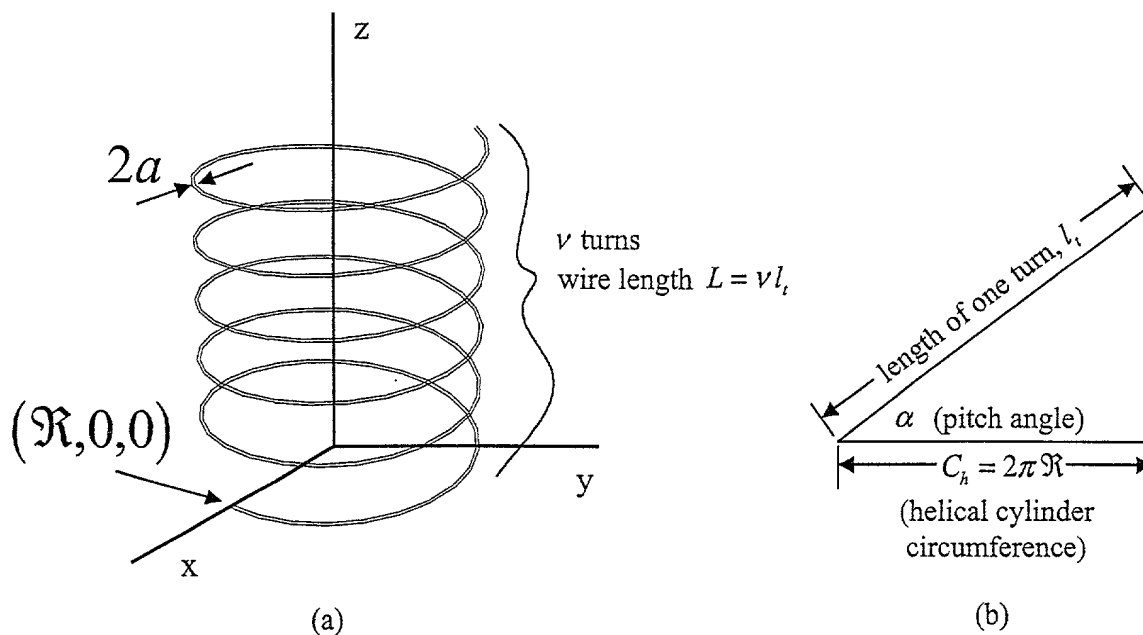

(a)   (b)

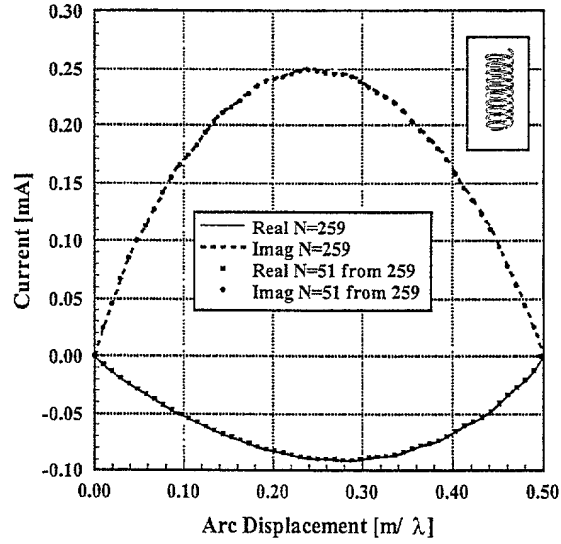Fig. 20. (a) Helical geometry, (b) additional definitions of helical parameters.

Fig. 21. Current on helix illuminated by plane wave, $\mathbf{E} = \left(\hat{\mathbf{x}}\cos\theta + \hat{\mathbf{z}}\sin\theta\right)e^{-jk(x\sin\theta - z\cos\theta)}$, ($\theta = 45°$, $L = 0.5\lambda$, $v = 10$, $\alpha = 20°$, $a = 0.0005\lambda$).
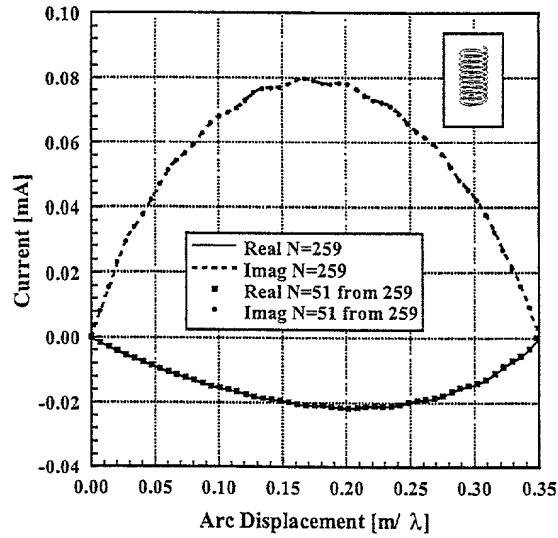

Fig. 22. Current on helix illuminated by plane wave, $\mathbf{E} = \left(\hat{\mathbf{x}}\cos\theta + \hat{\mathbf{z}}\sin\theta\right)e^{-jk(x\sin\theta - z\cos\theta)}$, ($\theta = 45°$, $L = 0.35\lambda$, $v = 10$, $\alpha = 20°$, $a = 0.0005\lambda$).
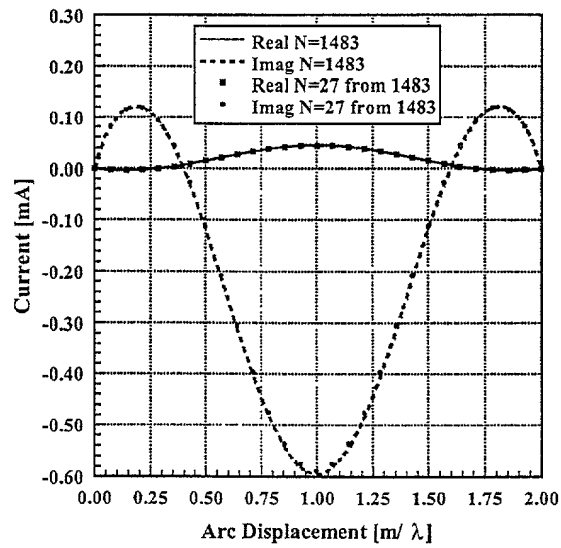
Fig. 23. Current on helix illuminated by plane wave, $\mathbf{E} = \hat{z}e^{-jkx}$ ($L = 2\lambda$, $v = 50$, $\alpha = 20°$, $a = 0.0005\lambda$).
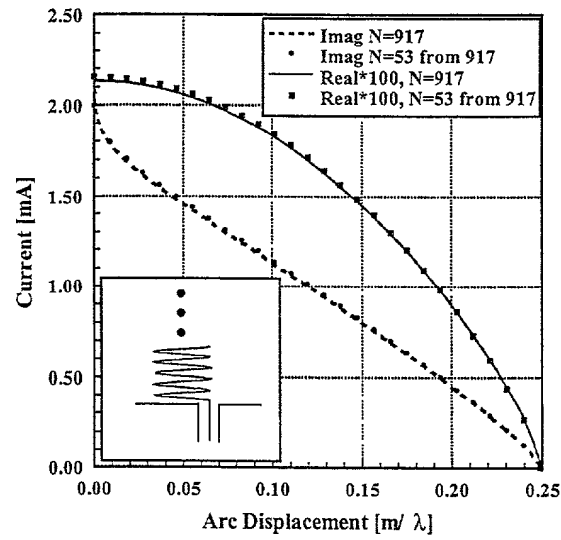

Fig. 24. Current on helix driven by delta-gap source ($L = 0.25\lambda$, $v = 25$, $\alpha = 20°$, $a = 0.0005\lambda$).

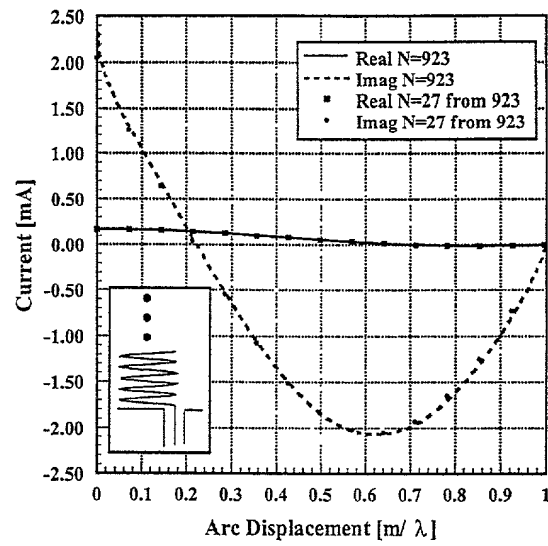Fig. 25. Current on helix driven by delta-gap source ($L = \lambda$, $v = 25$, $\alpha = 20°$, $a = 0.0005\lambda$).
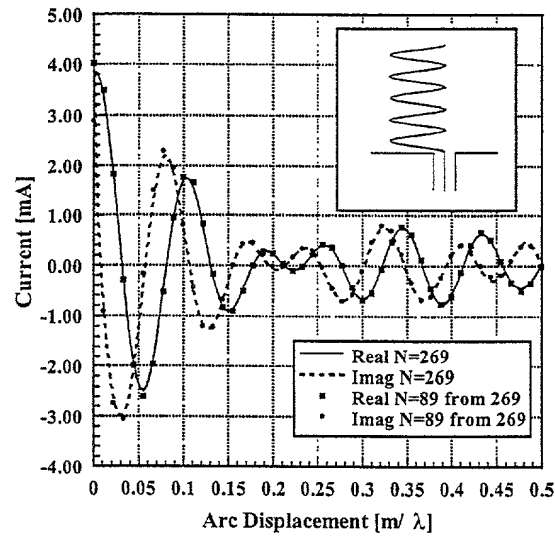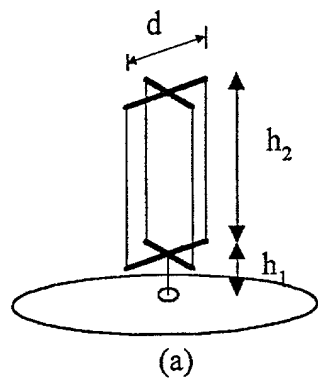

Fig. 26. Current on helical antenna driven by delta-gap source ($L = 0.5\lambda$, $C_h = 0.1\lambda$, $\alpha = 12.5°$, $a = 0.005\lambda$).

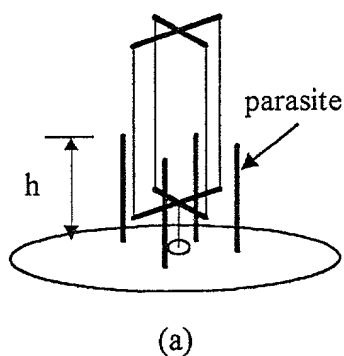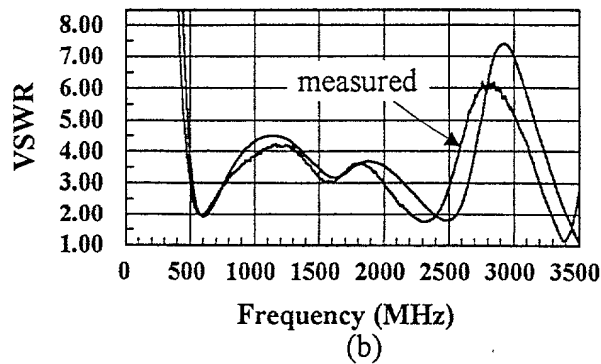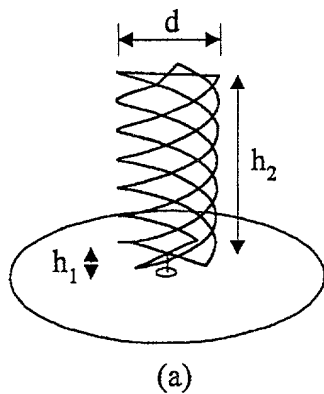| wire radius	0.814 mm
h_1	1.2 cm
h_2	16 cm
d	2.2 cm
strip width	3.256 mm
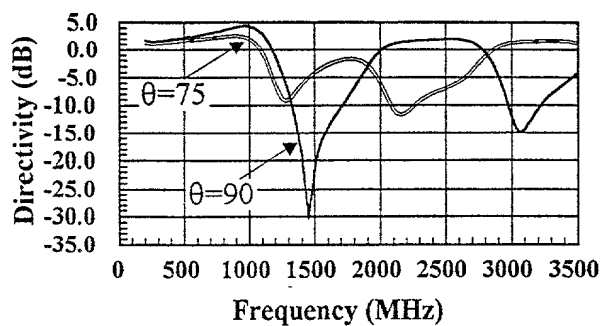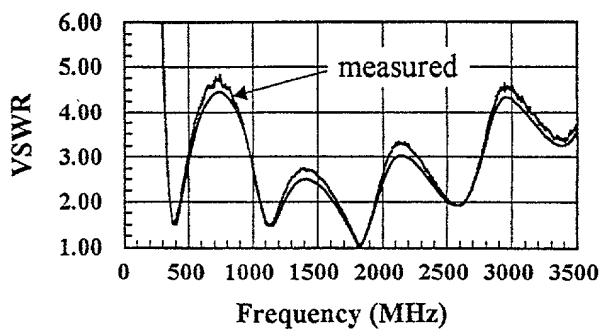
Fig. 101

(a) Cage monopole. (b) VSWR (c) Directivity.
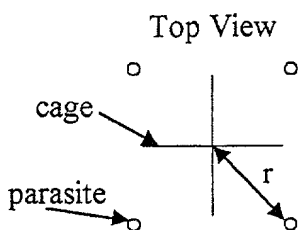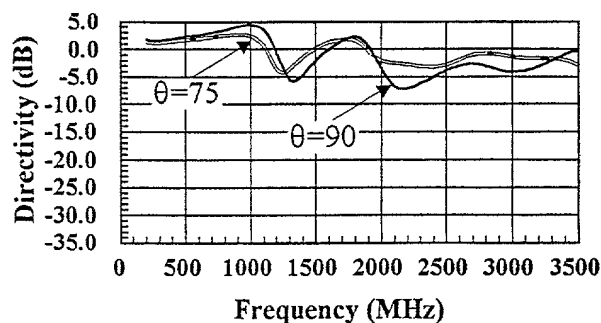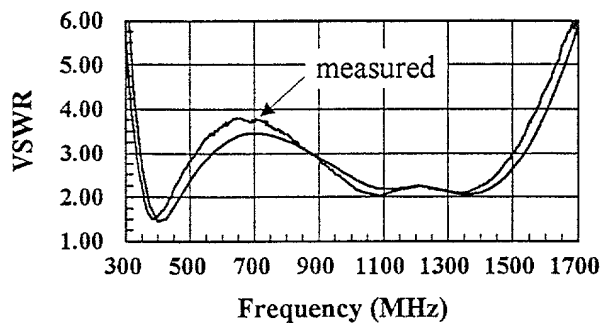
h	4.0 cm
r	2.5 cm

Fig. 102

(a) Sleeve-cage monopole. (Cage of Fig. 101a with parasites.) (b) VSWR. (c) Directivity.

Fig. 103

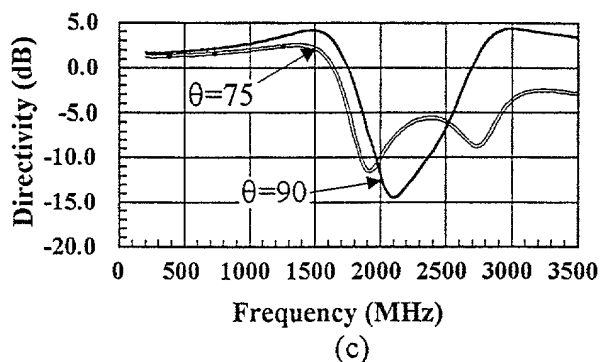| wire radius	0.814 mm
strip width	3.256 mm
length of wire per helix	13.2 cm
number of turns per helix	1.4
pitch angle	42°
h1	0.91 cm
h2	8.85 cm
d	2 cm

(a) Quadrifilar helix. (b) VSWR. (c) Directivity.

Top View

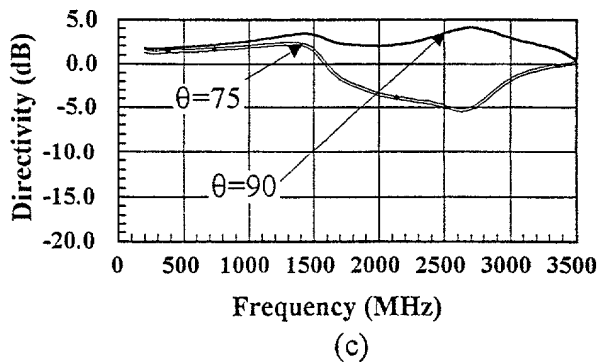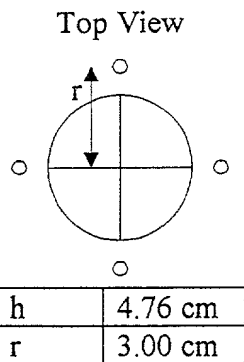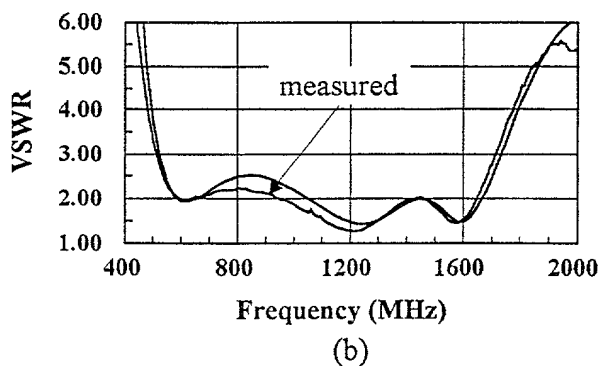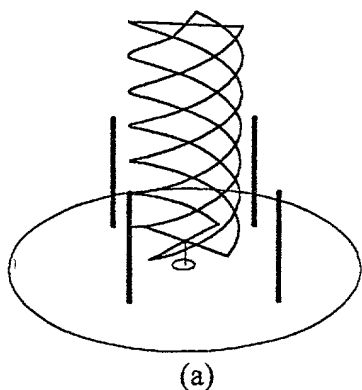| h	4.76 cm
r	3.00 cm

Fig. 104   (a) Sleeve helix. (Helix of Fig. 103a with parasites.) (b) VSWR. (c) Directivity.

Figure Captions

Fig. 201 Cage monopole.

Fig. 202 Characteristics of cage antenna optimized for VSWR < 2.0 ($a = 0.814$mm, $d = 4.7$ cm, $w = 3.4$ mm, $h_1 = 1$cm, $h_2 = 9.3$ cm, $Z_0 = 50\Omega$)

(a) VSWR

——— Computed
----- Measured

(b) input impedance.

——— Real (computed)
----- Imag (computed)
  + Real (measured)
  ◇ Imag (measured)

Fig. 203 Characteristics of cage antenna optimized for VSWR <2.5 ($a = 3.175$mm, $d = 8.2$ cm, $w = 12.7$mm, $h_1 = 2.55$cm, $h_2 = 24$ cm, $Z_0 = 50\Omega$)

(a) VSWR

········ straight wire (h=26.55cm, a=4.1 cm)
----- straight wire (h=26.55cm, a=3.175mm)
——— cage monopole

(b) directivity for $\phi = 0$.

——— $\theta = 90$
----- $\theta = 75$
········ $\theta = 60$

Table 201 Parameters and properties of cage dipoles, helical monopole (HX-MP) of (NAKANO, H., IKEDA, N., WU, Y., SUZUKI, R., MIMAKI, H., and YAMAUCHI, J.: 'Realization of dual-frequency and wide-band VSWR performances using normal-mode helical and inverted-F antennas', *IEEE Trans. Antennas Propagat.*, June 1998, 46, (6), pp. 788-793) Fig. 2c, and sleeve dipole of (KING, H.E., and WONG, J.L.: 'An experimental study of a balun-fed open-sleeve dipole in front of a metallic reflector', *IEEE Trans. Antennas Propagat.*, March 1972, 20, (2), pp. 201-204) Fig 2.
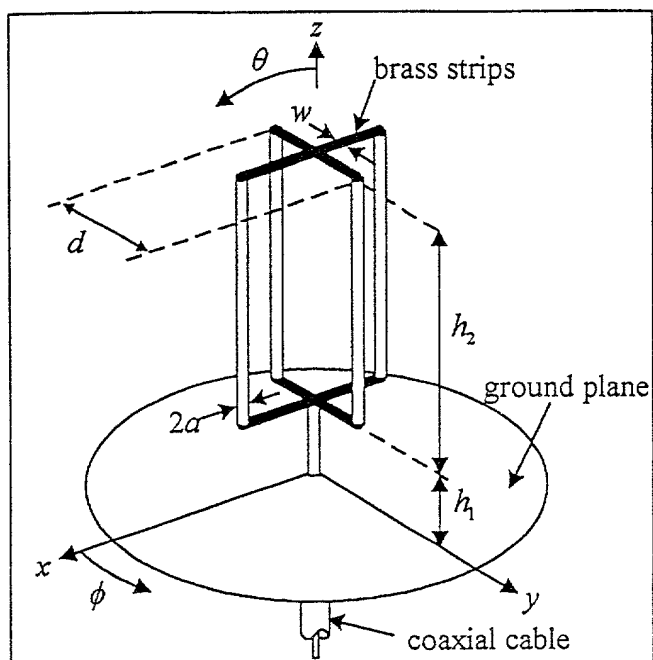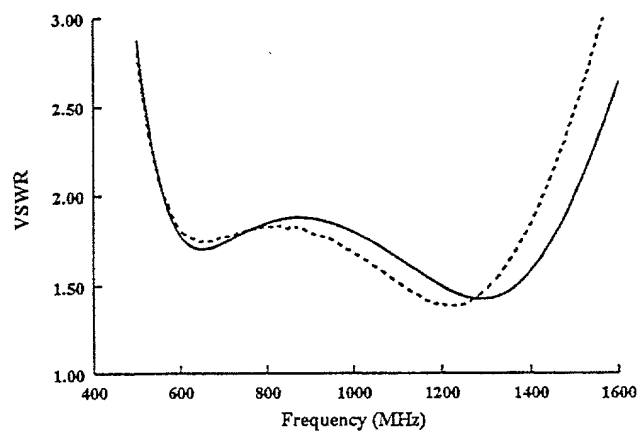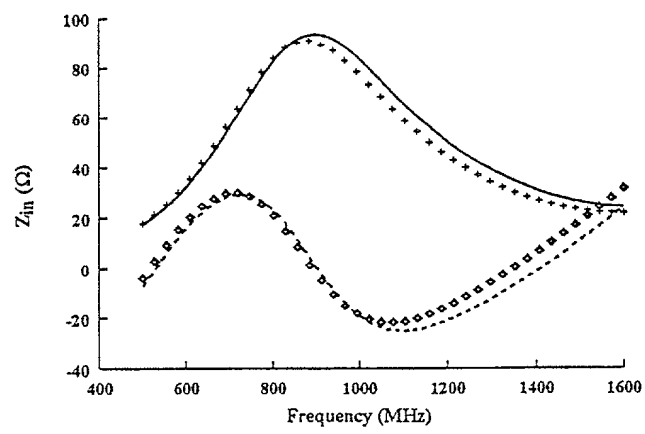
Fig. 201

Fig. 202 (a),(b)
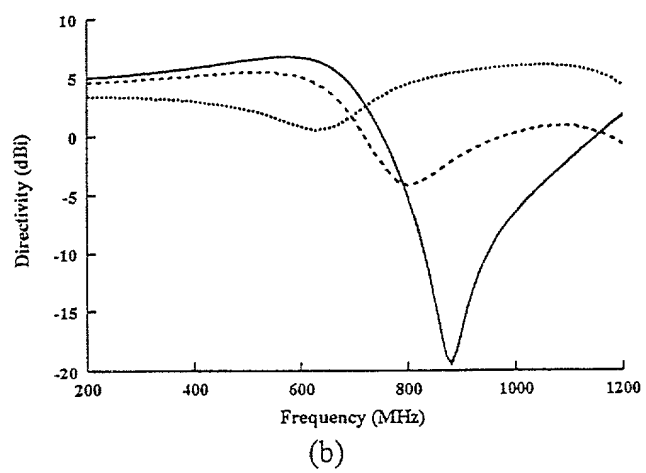

(a)

(b)

Fig. 203(a),(b)

(a)

(b)
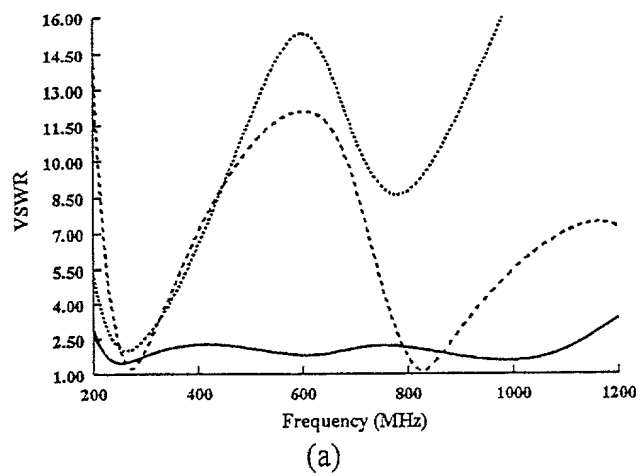
Table 201

Structure	Cage (Fig. 202)	HX-MP	Cage (Fig. 203)	Sleeve Dipole
VSWR	< 2	< 3.5	< 2.5	< 2.5
bandwidth ratio	2.6	1.7	5.4	1.8
f (MHz)	575-1500	627-1048	210-1130	225-400
height (cm)	10.3	19.8	26.55	51
width (cm)	4.7	0.47	8.2	13
wire radius (mm)	0.814	0.3	3.175	14.3

Fig. 201 (unlettered)
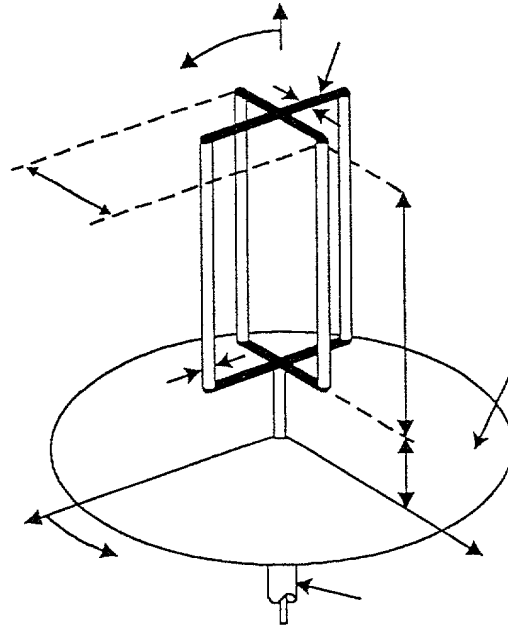
Fig. 201 (without arrows or letters)

Fig. 202a (unlettered)

Fig. 2.02b (unlettered)

Fig. 203 ·a (unlettered)

Fig. 203 b (unlettered)

Fig. 301 (a) Cage monopole antenna ($a = 0.814$mm, $d = 2.2$cm, $w = 3.256$mm, $h_1 = 1.2$cm, $h_2 = 16$cm, $Z_0 = 50\Omega$), (b) Measured and computed VSWR of cage monopole and straight wire of same radius, (c) Measured and computed input impedance, (d) Computed directivity ($\phi = 0$).
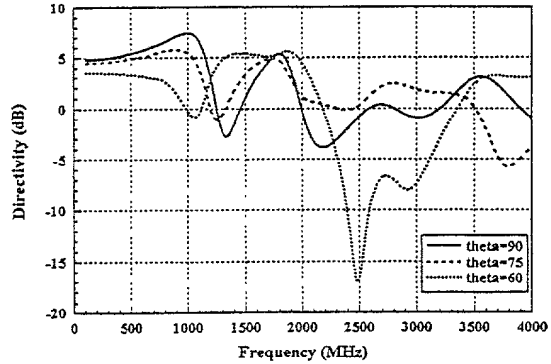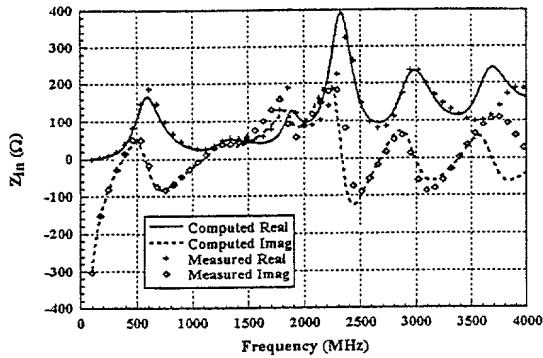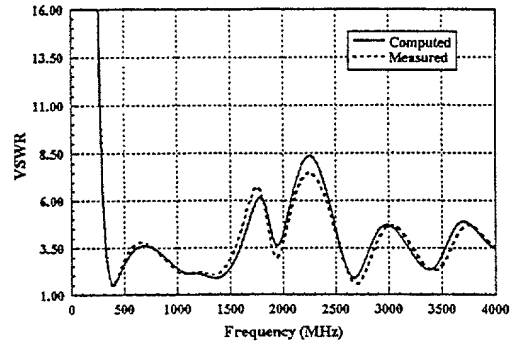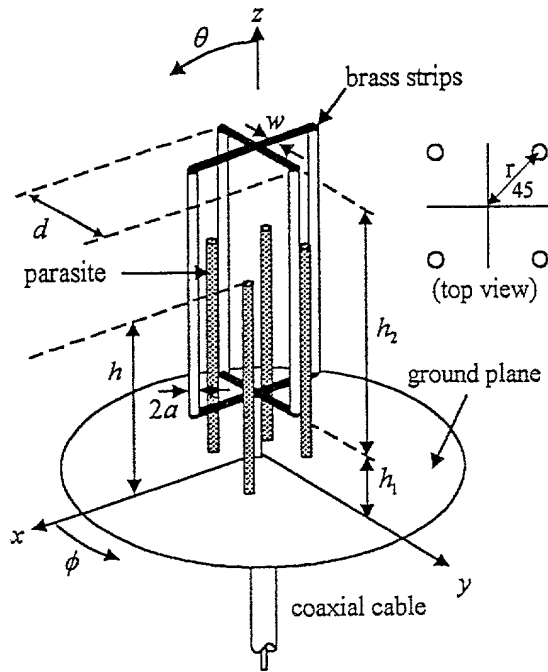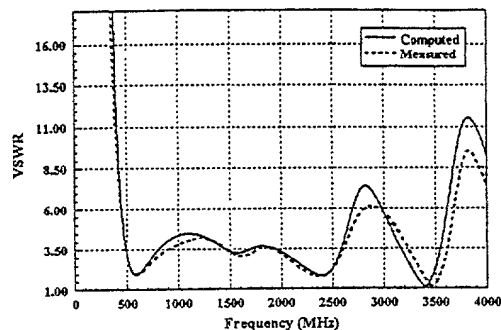
Fig. 302 (a) Sleeve-cage monopole antenna ($a = 0.814$mm, $d = 2.2$cm, $w = 3.256$mm, $h_1 = 1.2$cm, $h_2 = 16$cm, $r = 2.5$cm, $h = 4$cm, $Z_0 = 50\Omega$), (b) Measured and computed VSWR of sleeve-cage, (c) Measured and computed input impedance, (d) Computed directivity ($\phi = 0$).
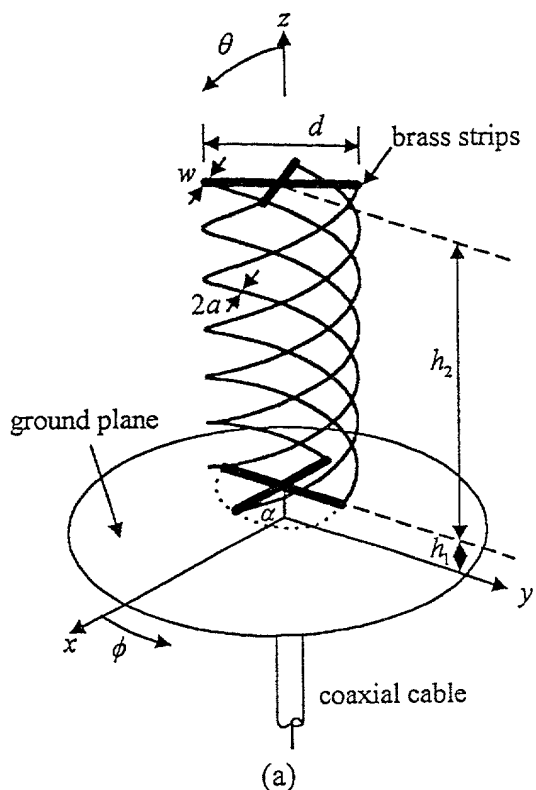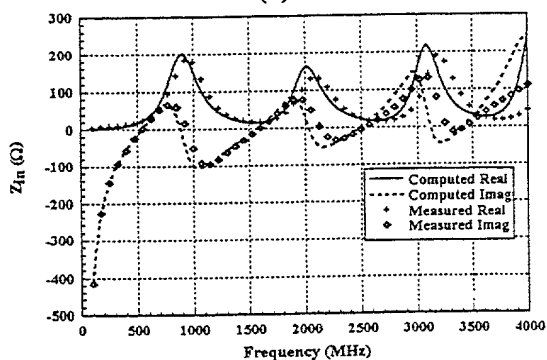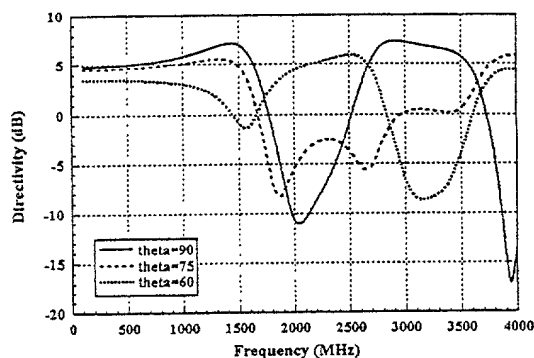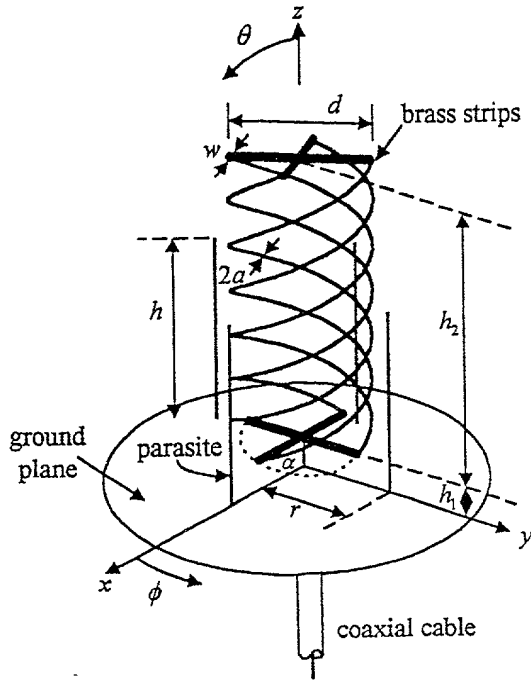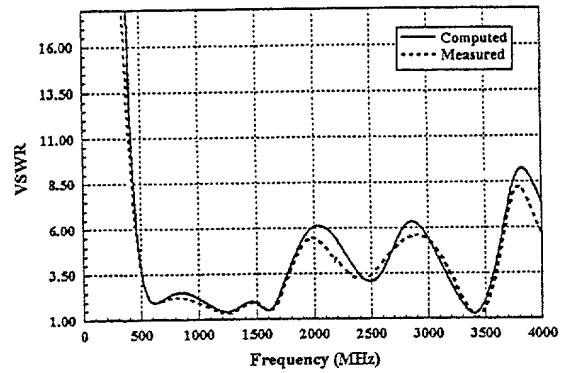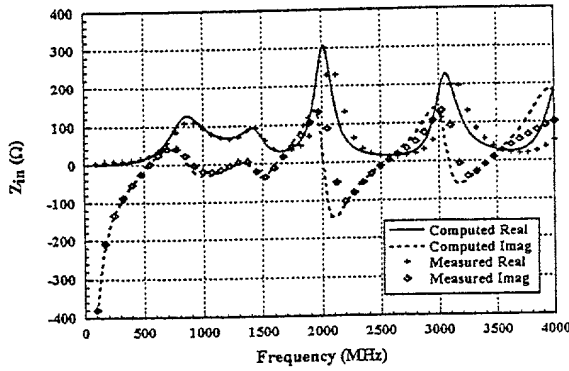
Fig. 303 (a) Quadrifilar helical antenna ($a = 0.814$mm, $d = 2$cm, $w = 3.256$mm, $h_1 = 0.91$cm, $h_2 = 8.85$cm, $Z_0 = 50\Omega$), (b) Measured and computed VSWR, (c) Measured and computed input impedance, (d) Computed directivity ($\phi = 0$).

Fig. 304 (a) Sleeve helical antenna ($a = 0.814$mm, $d = 2$cm, $w = 3.256$mm, $h_1 = 0.91$cm, $h_2 = 8.85$cm, $r = 3$cm, $h = 4.76$cm, $Z_0 = 50\Omega$), (b) Measured and computed VSWR, (c) Measured and computed input impedance, (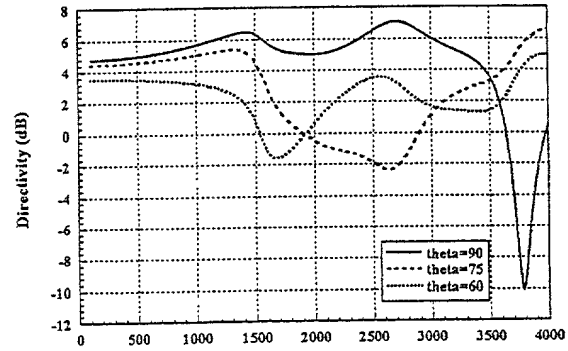d) Computed directivity ($\phi = 0$).